HHS Public Access

Author manuscript

J Immunol. Author manuscript; available in PMC 2022 February 15.

Published in final edited form as:

J Immunol. 2021 February 15; 206(4): 797–806. doi:10.4049/jimmunol.2000091.

Inhibition of efferocytosis by eCIRP-induced neutrophil extracellular traps

Kehong Chen[1], **Atsushi Murao**[1], **Adnan Arif**[1], **Satoshi Takizawa**[1], **Hui Jin**[1], **Jianxin Jiang**[2], **Monowar Aziz**[1,*,†], **Ping Wang**[1,3,*,†]

[1]Center for Immunology and Inflammation, The Feinstein Institutes for Medical Research, Manhasset, New York.

[2]State Key Laboratory of Trauma, Burns and Combined Injury, Institute of Surgery Research, Daping Hospital, Chongqing, China.

[3]Department of Surgery, Donald and Barbara Zucker School of Medicine at Hofstra/Northwell, Manhasset, New York.

Abstract

Phagocytic clearance of apoptotic cells by the macrophages (efferocytosis) is impaired in sepsis, but its mechanism is poorly understood. Extracellular cold-inducible RNA-binding protein (eCIRP) is a novel damage-associated molecular pattern (DAMP) which fuels inflammation. We identify that eCIRP-induced neutrophil extracellular traps (NETs) impair efferocytosis through a novel mechanism. Co-culture of macrophages and apoptotic thymocytes in the presence of recombinant murine (rm) CIRP-induced NETs significantly inhibited efferocytosis. Efferocytosis was significantly inhibited in the presence of rmCIRP-treated wild-type (WT), but not PAD4$^{-/-}$ neutrophils. Efferocytosis in the peritoneal cavity of rmCIRP-injected PAD4$^{-/-}$ mice was higher than WT mice. Milk fat globule-EGF-factor VIII (MFG-E8) increased macrophage efferocytosis, while the inhibition of efferocytosis by NETs was not rescued upon addition of MFG-E8, indicating disruption of MFG-E8's receptor(s) $\alpha_v\beta_3$ or $\alpha_v\beta_5$ integrin by the NETs. We identified neutrophil elastase (NE) in the NETs significantly inhibited efferocytosis by cleaving macrophage surface integrins $\alpha_v\beta_3$ and $\alpha_v\beta_5$. Using a pre-clinical model of sepsis, we found that CIRP$^{-/-}$ mice exhibited significantly increased rate of efferocytosis in the peritoneal cavity compared to WT mice. We discovered a novel role of eCIRP-induced NETs to inhibit efferocytosis by the NE-dependent decrease of $\alpha_v\beta_3/\alpha_v\beta_5$ integrins in macrophages. Targeting eCIRP ameliorates sepsis by enhancing efferocytosis.

[*]**Address for correspondence:** Monowar Aziz, PhD, Assistant Professor, Center for Immunology and Inflammation, The Feinstein Institute for Medical Research, 350 Community Dr., Manhasset, NY 11030, Tel: (516) 562-2436, Fax: (516) 562-2396, Maziz1@northwell.edu, Ping Wang, MD, Professor and Chief Scientific Officer (CSO), The Feinstein Institutes for Medical Research, 350 Community Dr., Manhasset, NY 11030, Tel: (516) 562-3411, Fax: (516) 562-2396, Pwang@northwell.edu.

Author contributions

KC and MA designed the experiments. KC, AA performed all *in vivo* works. KC, AM, AA, ST, HJ performed phagocytosis assay, flow cytometry, microscopy and NETs assay. KC, JJ, MA analyzed the data. KC, MA, AA prepared the figures. MA wrote the manuscript. PW revised the manuscript. PW, MA conceived the concept of this study. MA and PW supervised the work.

[†]Contributed equally to this work

Keywords

eCIRP; NETs; Efferocytosis; MFG-E8; Neutrophil Elastase; Apoptotic Cells; Integrin

Introduction

Sepsis is a life-threatening inflammatory condition caused by body's exaggerated immune response to an infection(1). Besides cytokine storm initiated by the interaction of pathogen-associated molecular patterns (PAMPs) or damage-associated molecular patterns (DAMPs) with the pattern recognition receptors (PRRs)(2), sepsis is characterized by increased cellular apoptosis(3). Phagocytic clearance of apoptotic cells by the macrophages, also known as efferocytosis plays an important role in resolving inflammation(4, 5). Unengulfed apoptotic cells may undergo secondary necrosis and spill over intracellular noxious substances called DAMPs to exaggerate inflammation and organ injury(4, 6). Although the impaired efferocytosis is one of the hallmarks of several inflammatory/autoimmune diseases, the causes and mechanisms of impairment in efferocytosis are less understood.

Apoptotic cells release "find me" signals such as fractalkine (CX3CL1), lysophosphatidylcholine, and sphingosine-1-phosphate to attract and activate phagocytes(7, 8). Apoptotic cells express "eat me" signal phosphatidylserine (PS) on their surface to be recognized by the phagocytes(7, 9). Milk fat globule-EGF-factor VIII (MFG-E8) is a secretory glycoprotein, which binds $\alpha_v\beta_3/\alpha_v\beta_5$ integrin on phagocytes through its N-terminal domains and eat-me signal on the apoptotic cells through its C-terminal domains and links phagocytes and apoptotic cells(10, 11). Phagocytes then undergo cytoskeletal rearrangements to internalize apoptotic cells, process ingested dead cells, and release anti-inflammatory mediators to control inflammation(5, 7).

Cold-inducible RNA-binding protein (CIRP) is a 18-kDa RNA chaperone protein(12). CIRP is released extracellularly during sepsis, hemorrhagic shock or ischemia-reperfusion (I/R) injuries through passive release from necrotic cells or actively through lysosomal exocytosis pathway(13). Extracellular CIRP (eCIRP) binds Toll-like receptor 4 (TLR4) and induces macrophages to release pro-inflammatory cytokines (TNF-α, IL-6, IL-1β) and chemokines (KC, MIP-2), exaggerating inflammation and tissue injury in sepsis(13). Elevated plasma level of eCIRP is correlated with a poor prognosis in patients with shock(13). Being a new DAMP, a detailed knowledge about eCIRP's pathobiology in inflammatory diseases is needed to develop novel therapeutics.

Neutrophils provide a first line of defense against infection. Effector functions of neutrophils are mediated through the formation of neutrophil extracellular traps (NETs)(14). NETs are web-like extracellular chromatin coated with citrulinated histone 3 (citH3), myeloperoxidase (MPO), and neutrophil elastase (NE)(14). NETs trap and kill bacteria, but elevated production of NETs or continued presence of NET-forming neutrophils can cause excessive inflammation and tissue damage(15). NADPH-dependent production of reactive oxygen species (ROS) promote NET formation. ROS causes increased Ca^{++} influx and peptidyl arginine deaminase 4 (PAD4) activation. PAD4 converts arginine to citrulline in H3, leading to chromatin decondensation(16). NE and MPO are transported from azurophilic granules to

the nucleus to cleave linker histone H1 and modify the core histones. MPO also intensifies chromatin decondensation, through the synthesis of hypochlorous acid(16). Finally, chromatin is released outside the cells through membrane pores and cellular lysis as well as the activation of a pore forming protein gasdermin D (GSDMD)(17).

NETs are induced by a variety of stimuli such as, phorbol myristate acetate (PMA), endotoxin, cytokines, bacteria, virus, and fungi(14, 18). We have recently discovered that eCIRP increases NET formation *in vivo* and *in vitro* through the activation of PAD4(19). eCIRP induces the generation of a distinct type of neutrophils, ICAM-1^+ neutrophils which produce increased amount of NETs(20). Although eCIRP's role in NET formation has been demonstrated, the impact of NETs on macrophage functions in a clinically relevant condition has not been studied.

In this study, we discovered a previously unknown function of eCIRP-induced NETs to impede efferocytosis through a novel pathway. The presence of MFG-E8 was not able to reverse the impaired efferocytosis caused by NETs. Finally, we revealed that NE, a component of NETs cleaved MFG-E8's receptors $\alpha_v\beta_3$ and $\alpha_v\beta_5$ integrins in macrophages, leading to decreased efferocytosis. These findings uncovered the novel mechanism of NET-dependent impairment of efferocytosis, elucidated a potential role of eCIRP on effecrocytosis through NET formation, and directed a novel therapeutic avenue to correct the impaired efferocytosis by targeting eCIRP in sepsis.

Materials and Methods

Mice

Male, 8–10 week old wild-type (WT) C57BL/6 mice were purchased from Charles River Laboratories (Wilmington, MA). B6.Cg-*Padi4*$^{tm1.1Kmow}$/J or $PAD4^{-/-}$ mice were purchased from The Jackson Laboratory (Stock No.: 030315; Bar Harbor, ME). C57BL/6 $CIRP^{-/-}$ mice were obtained from Dr. Jun Fujita (Kyoto University, Kyoto, Japan). Age-matched mice were used for all experiments. Mice were housed in temperature (~23°C) controlled rooms with 12 h light cycles and provided standard laboratory chow and drinking water. All experiments were performed in accordance with the guidelines for the use of experimental animals by National Institutes of Health (Bethesda, MD). All the experiments involving mice were approved (protocol # 2018–026) by the Institutional Animal Care and Use Committees (IACUC) of the Feinstein Institutes for Medical Research.

Sepsis model: Cecal ligation and puncture

Aged matched, male WT and $CIRP^{-/-}$ mice were anesthetized with inhaled isoflurane and placed in supine position. Cecal ligation and puncture (CLP) was preformed through a midline laparotomy. Briefly, the abdomen was shaved and disinfected. A 2-cm incision was created, the cecum was exposed, and ligated with a 4–0 silk suture 1 cm proximal from the distal cecal extremity. The cecum was punctured twice with a 22-guage needle. A small amount of cecal content was extruded and the ligated cecum was returned to the peritoneal cavity. The wound was closed in layers. Sham animals underwent a laparotomy without

cecal ligation or puncture. After closure, the mice received a subcutaneous injection of 1 ml of normal saline to avoid stress-induced dehydration.

Isolation of thymocytes and induction of apoptosis

Thymus was removed from C57BL/6 WT mice and mechanically disrupted between two frosted glass slides in 10 mL RPMI Medium 1640 (1×) supplemented with 10 μM/L HEPES, 2 mM/L of L-glutamine, 50 μM/L 2-mercaptoethanol, 100 units/mL penicillin, 100 μg/mL streptomycin, purchased from Gibco, Life Technologies Limited, Paisley, PA4 9RF, UK, and 10% fetal bovine serum (FBS; MP Biomedicals, Solon, OH). Freshly prepared thymocytes were washed with PBS and were distributed in 6-well plates (2×10^6 cells/well) in 2 mL RPMI 1640 complete medium and placed in a 37 °C humidified incubator with 5% CO_2 in air. After 1 h, thymocytes were treated with dexamethasone (10 μM) for 5 h to induce apoptosis. Thymocytes were then stained with Annexin V-Fluorescein isothiocyanate (FITC) and propidium iodide (PI) (BD Biosciences, San Jose, CA) and apoptosis was assessed by a BD LSR Fortessa Flow Cytometry Analyzer (BD Biosciences) and the data were analyzed by FlowJo software (Tree Star, Ashland, OR).

Isolation and culture of peritoneal macrophages

Peritoneal macrophages were isolated from C57BL/6 mice as described previously(21). Briefly, 1 mL of 3% thioglycolate (Sigma Aldrich, St. Louis, MO) was injected in mice intraperitoneally. Four days later, mice were euthanized using CO_2 asphyxiation. Peritoneal fluids were isolated using peritoneal lavage with PBS. Total peritoneal cells were enriched by centrifugation at 300 ×g for 10 min and cultured in RPMI 1640 medium (Gibco). After 3 h nonadherent cells were removed and adherent cells, mainly the primarily macrophages, were cultured overnight prior to use. All cultured media was supplemented with 10% heat-inactivated FBS (MP Biomedicals), 1% penicillin-streptomycin and 2 mM glutamine. Cells were maintained in a humidified incubator with 5% CO_2 at 37 °C.

Isolation and purification of bone marrow-derived neutrophils

Bone marrow-derived neutrophils (BMDN) were isolated from WT and PAD4$^{-/-}$ mice as described previously(19). Mice were anesthetized by 2% isoflurane inhalation and the femurs and tibias were dissected. Bone marrow contents were flushed out with Ca^{++} and Mg^{++} free Hank's Balanced Salt Solution (HBSS; Mediatech Inc., Manassas, VA) into a 10-cm petri dish using a 25 gauge needle. Cell suspensions were filtered through a 70 μm cell strainer (Corning Life Sciences, Teterboro, NJ) and BMDN were purified by negative selection using the EasySep mouse neutrophil enrichment kit (Cat No.: 19762 and 18000; STEMCELL, Vancouver, Canada). The purity of sorted neutrophils was checked by staining the cells with Ly6G (clone 1A8, Biolegend, San Diego, CA) and CD11b (clone M1/70, Biolegend) Abs using BD LSR Fortessa flow cytometer (BD Biosciences).

Isolation of rmCIRP-induced NETs

Recombinant murine (rm) CIRP was prepared in-house as described previously(13). A total of 5×10^6 BMDN were stimulated with various doses of rmCIRP for 4 h at 37 °C in a 6-well culture plate in 5% CO_2 humidified incubator. After 4 h of stimulation with rmCIRP,

media containing the floating BMDN were gently aspirated and discarded, leaving the layer of NETs and neutrophils adhered at the bottom. Using a total of 1.5 mL of cold PBS without Ca^{++} and Mg^{++} the bottom of each well was washed in order to lift off all adherent materials from the bottom, and collected the liquids containing NETs in a 1.5 mL micro-centrifuge tube and centrifuged for 10 min at 300 ×g at 4 °C. After centrifugation, neutrophils and any remaining cells were pelleted at the bottom, leaving a cell-free NET-rich supernatant, which was then collected into a 1.5 mL micro-centrifuge tubes, and centrifuged at 18,000 ×g for 10 min at 4 °C. Discard supernatant and suspend all pellets obtained together in 100 μl of ice cold PBS. Measure DNA concentration in the sample obtained using a NanoDrop ND-1000 spectrophotometer (Thermo Scientific).

Assessment of NETs by ELISA

BMDN (5×10^6) were stimulated with various doses of rmCIRP for 4 h at 37 °C in a 6-well culture plate in 5% CO_2 humidified incubator. Crude NETs extracts were isolated as described above, sonicated, diluted in PBS, and 100 μl of each sample was loaded into anti-MPO Ab (clone: mAb 8F4; Hycult Biotech, Uden, The Netherlands) coated plate. For generating standard curve DNA concentration in one of the rmCIRP-treated samples was measured, serially diluted and loaded in the anti-MPO Ab-coated ELISA plate. Plate was incubated at room temperature for 2 h. After that plate was washed with PBS, reacted with anti-DNA-POD Ab (Cell Death Detection Kit, Cat. No. 11 544 675 001, Roche Diagnostics, GmbH, Mannheim, Germany) and subsequently the optical density was recorded at 405 nm after adding TMB substrate to each well. NETs in context of its NE-DNA contents were expressed as ng/mL/5×10^6 cells.

In vitro phagocytosis assay by flow cytometry

Peritoneal macrophages were plated at a density of 5×10^5 cells in 24 well plate. Just before phagocytosis assay, the macrophages were washed three times with fresh serum-free RPMI 1640 medium. Mouse thymocytes were labeled using a Vybrant™ CFDA SE Cell Tracer Kit (V12883) by following the manufacturer's instructions (Molecular Probes, Eugene, OR). Carboxyfluorescein diacetate succinimidyl ester (CFSE)-labeled thymocytes were induced apoptosis by dexamethasone (10 μM; Millipore Sigma, St. Louis, MO) treatment for 5 h as described above. In order to perform phagocytosis assay, CFSE-labeled apoptotic thymocytes (1.5×10^6 cells) suspended in 500 μl RPMI 1640 medium were added to each well of a 24-well plate containing macrophage monolayers in presence of different doses of NETs (1–1000 ng/mL) or recombinant human (rh) NE (10–1000 ng/mL, 9167-SE, R&D Systems, Minneapolis, MN) with or without 100 μM NE inhibitor Sivelestat Sodium (Selleck Chemical LLC, 50-136-6316, Houston, TX) and incubated at 37°C for 60 min. Non-ingested cells were removed by washing three times with ice-cold phosphate buffered saline (PBS). Cells were collected by scrapping and stained in PBS containing 1% albumin with PE- or APC-conjugated F4/80 (BM8; BioLegend, San Diego, CA) Ab at room-temperature (RT) for 15 min. The phagocytosis of apoptotic thymocytes by the macrophages were presented as the frequencies (%) of FITC positive cells within PE- or APC-conjugated F4/80 positive cells (macrophages) by flow cytometry.

In vivo phagocytosis assay

Recombinant mouse CIRP (rmCIRP) was produced in our lab as previously described(13). rmCIRP at a dose of 5 mg/kg BW or normal saline was administered intraperitoneally (*i.p.*). At 5 h after rmCIRP injection, 1×10^7 CFSE-labeled apoptotic thymocytes were injected *i.p.* into WT and PAD4 $^{-/-}$ mice. After 1 h of injection, mice were sacrificed and peritoneal exudate cells were harvested by peritoneal lavage with 8–10 mL PBS. Efferocytosis of apoptotic thymocytes by macrophages were presented as the percentage of FITC positive cells in APC-conjugated F4/80 positive cells by flow cytometry.

WT or PAD4 $^{-/-}$ neutrophil, macrophage and thymocytes co-culture

A total of 1×10^6 BMDN from WT or PAD4$^{-/-}$ mice were stimulated with 1 μg/mL of rmCIRP for 4 h at 37 °C in a 24-well plate in 5% CO_2 humidified incubator. After 4 h of stimulation, supernatants were gently aspirated and discarded, leaving the layers of NETs and neutrophils adhered at the bottom. A total of 5×10^5 peritoneal macrophages were added into these WT and PAD4$^{-/-}$ PMN containing 24-well plates. After 2 h at 37°C, the macrophages were gently washed three times with fresh serum-free medium. Approximately, 1.5×10^6 CFSE-labeled apoptotic thymocytes were added into each well of the 24-well plate followed by incubation at 37°C for 60 min. Non-ingested cells were removed by washing three times with ice-cold PBS. Cells were collected and stained with PE or APC-conjugated F4/80 Ab (BioLegend) for flow cytometry.

Assessment of $\alpha_v\beta_3$ and $\alpha_v\beta_5$ integrin expression in macrophages by flow cytometry

To detect integrin $\alpha_v\beta_3$ and integrin $\alpha_v\beta_5$ expression on the surface of macrophages, a total of 1×10^6 primary peritoneal macrophages were washed with FACS buffer containing PBS with 2% FBS and stained with Alexa Fluor 700 anti-mouse integrin α_v Ab (clone: 235112, R&D systems) and Alexa Fluor 647 anti-mouse integrin β_3 Ab (clone: 909114, R&D systems) or PE anti-mouse integrin β_5 Ab (14–0497, eBioscience). Unstained cells were used as a negative control to establish the flow cytometer voltage setting. Acquisition was performed on 10,000 events using a BD LSR Fortessa flow cytometer (BD Biosciences) and data were analyzed with FlowJo software (Tree Star, Ashland, OR).

Immunofluorescence assay

After co-culture of CFSE-labeled apoptotic thymocytes and peritoneal macrophages for 1 h, non-ingested cells were removed by washing 3 times with ice-cold PBS. The cells were incubated with 2% paraformaldehyde solution for 20 min at RT and then washed with PBS and blocked with normal 5% normal horse serum for 1 h. PE-conjugated rat anti-mouse F4/80 Ab were diluted in 1% horse serum and incubated with cells for 2 h in the dark at room temperature. Confocal microscopy images were obtained at using a Zeiss LSM880 confocal microscope equipped with a 40× objective (White Plains, NY).

Real-time quantitative reverse transcription polymerase chain reaction (RTqPCR)

Total RNA was extracted from a total of 5×10^5 peritoneal macrophages stimulated with NETs (1000 ng/mL) or rhNE (1000 ng/mL) for 1 h. After stimulation of the cells with NETs or rhNE, mRNA was isolated using Trizol reagent (Invitrogen, Carlsbad, CA) and assessed

the expression of integrins α_v, β_3, β_5 using RTqPCR. cDNA was synthesized using MLV reverse transcriptase (Applied Biosystems, Foster City, CA). PCR reactions were carried out in 20 μl of a final volume of 0.08 μM of each forward and reverse primer (Supplemental Table 1), cDNA, water, and SYBR Green PCR master mix (Applied Biosystems). Amplification and analysis was conducted in a Step One Plus real-time PCR machine (Applied Biosystems). Mouse β-actin mRNA was used as an internal control for amplification and relative gene expression levels were calculated using the ΔΔCT method. Relative expression of mRNA was expressed as fold change in comparison with PBS-treated cells.

Statistical analysis

Data represented in the figures are expressed as mean ± SEM. ANOVA was used for one-way comparison among multiple groups and the significance was determined by the Student–Newman–Keuls (SNK) test or the Tukey method, as appropriate. The paired Student *t* test was applied for two-group comparisons. Significance was considered for $p \leq 0.05$ between study groups. Data analyses were carried out using GraphPad Prism graphing and statistical software (GraphPad Software, San Diego, CA).

Results

eCIRP induces NETs to inhibit macrophage efferocytosis

We first determined eCIRP-mediated induction of NET formation. Stimulation of bone marrow-derived neutrophil(s) (BMDN) with rmCIRP significantly induced NET formation in a dose-dependent manner compared to rmCIRP non-treated cells (Supplemental Fig. 1A, B). Microscopically, the rmCIRP-treated BMDN showed web-like chromatin structures and cell swelling, indicating NET formation, which were absent in PBS-treated BMDN (Supplemental Fig. 1C). We then determined the effect of eCIRP-induced NETs on efferocytosis. We extracted NETs from rmCIRP-treated BMDN and quantified by its extracellular DNA contents. *Treatment* of *thymocytes* with *dexamethasone in vitro induced apoptosis* in a large fraction of the *cells* (~60%) by 5 *h* (Supplemental Fig. 1D, E). We cultured peritoneal macrophages with apoptotic thymocytes in the presence of various doses of NETs. Addition of eCIRP-induced NETs to the macrophage and apoptotic cell cultures significantly inhibited macrophage efferocytosis in a dose-dependent manner at 0.5 (Supplemental Fig. 1F) and 1 h compared to without NETs treated condition (Fig. 1A, B). In the F4/80 vs FSC zebra blot of Fig. 1A, we indicated that 43.1% (PBS-treated group) were the cells in the gate respect to the total cells into the region selected in SSC vs FSC blot. In the CFSE vs FSC blot, the 36.2% (PBS-treated group) was calculated as the number of cells in the region considering 100% the positive gate for F4/80. These data clearly indicate that eCIRP-induced NETs inhibit efferocytosis. Image stream data also confirmed the engulfment of apoptotic cells by the macrophages as depicted by the co-localization of CFSE-labeled green cells with F4/80 positive red macrophages (Fig. 1C). We further examined the effects of PMA-induced NETs on efferocytosis. Akin to the inhibitory effects of eCIRP-induced NETs on efferocytosis, the PMA-induced NETs were also able to inhibit efferocytosis by 25% compared to PBS-treated control (Supplemental Fig. 1G, H).

eCIRP-induced wild-type, but not PAD4$^{-/-}$ neutrophils inhibit efferocytosis

Activation of PAD4 promotes NET formation (22). eCIRP induces PAD4 activation to form NETs(19). To investigate whether the inhibition of eCIRP-induced NET formation restores efferocytosis, we co-cultured peritoneal macrophages with apoptotic cells in the presence of neutrophils isolated from WT or PAD4$^{-/-}$ mice. We treated co-cultured cells with or without rmCIRP and assessed efferocytosis in macrophages. We found that in the absence of rmCIRP treatment, peritoneal macrophages showed similar outcomes in macrophage effereocytosis regardless of the presence of either WT or PAD4$^{-/-}$ neutrophils (Fig. 2A, B, Supplemental Fig. 2A). However, with rmCIRP treatment, peritoneal macrophages showed marked decrease in the macrophage efferocytosis in the presence of WT neutrophils. Conversely, upon rmCIRP treatment, peritoneal macrophages showed restoration in the inhibition of macrophage efferocytosis in the presence of PAD4$^{-/-}$ neutrophils compared to the presence of WT neutrophils (Fig. 2A, B, Supplemental Fig. 2A). Interestingly, there was no change in the macrophage efferocytosis with or without rmCIRP treatment in absence of neutrophils, indicating eCIRP alone cannot alter macrophage efferocytosis, it requires WT neutrophils to inhibit macrophage efferocytosis (Fig. 2A, B, Supplemental Fig. 2A).

To confirm these *in vitro* findings in mice, we injected WT and PAD4$^{-/-}$ mice with rmCIRP intraperitoneally to attract macrophages and neutrophils in the peritoneal cavity. We then injected fluorescent labeled WT apoptotic thymocytes in the peritoneal cavity and assessed macrophage efferocytosis. We found that injection of rmCIRP and apoptotic cells in the PAD4$^{-/-}$ mice showed significant increase in the macrophage efferocytosis compared to WT mice injected with rmCIRP and apoptotic cells intraperitoneally (Fig. 2C, D). These data suggest that NET-deficient neutrophils do not interfere with the macrophage efferocytosis after treatment with rmCIRP. Here, the efferocytosis within macrophages was determined by staining the cells with macrophage specific marker F4/80 that distinguishes macrophages from other cell populations present in the *in vitro* co-culture or peritoneal cavity. To exclude the possibility of discrepancies in cellular infiltration between rmCIRP treated WT and PAD4$^{-/-}$ mice for altering efferocytosis, we assessed the infiltration of macrophages and neutrophils in the peritoneal cavity after *i.p.* injection in WT and PAD4$^{-/-}$ mice with rmCIRP. We found that there were no significant difference in the frequencies and numbers of peritoneal macrophages and neutrophils between rmCIRP-treated WT and PAD4$^{-/-}$ mice (Fig. 2E, F, G, H, I, J, Supplemental Fig. 2B). After intraperitoneal injection of rmCIRP, we noticed significant amount of neutrophils were infiltrated into the peritoneal cavity. Under normal condition, considerable numbers of macrophages reside in the peritoneal cavity, while the neutrophils mainly reside in the bone marrow and blood. It is estimated that around 70% of the human and 30–50% of the mouse circulatory leukocytes are neutrophils, by contrast only 5% of the leukocytes in the blood are monocytes(23, 24). After rmCIRP injection into the peritoneal cavity, resident macrophages might release chemokines to attract more neutrophils into the peritoneal cavity. This gave rise to significantly increased numbers of total cells in the peritoneal cavity, which resulted in decreased % of peritoneal macrophages.

NETs inhibit $\alpha_v\beta_3/\alpha_v\beta_5$ integrin-dependent efferocytosis

MFG-E8 is an opsonin of apoptotic cells which increases efferocytosis(10). We found that treatment of macrophages with rmMFG-E8 increased efferocytosis, while treatment of macrophages with NETs decreased efferocytosis compared to PBS-treated control (Fig. 3A, B, Supplemental Fig. 2C). Intriguingly, we found that NET-induced inhibition of macrophage efferocytosis was not corrected even with MFG-E8 treatment to the culture (Fig. 3A, B, Supplemental Fig. 2C), indicating NETs may cause impairment of MFG-E8-mediated pathway for efficient engulfment of apoptotic cells by the macrophages. In phagocytic cells MFG-E8 binds $\alpha_v\beta_3$ or $\alpha_v\beta_5$ integrin(10). We assessed the surface expression of $\alpha_v\beta_3$ and $\alpha_v\beta_5$ integrins, and found that following treatment of macrophages with various doses of NETs the frequencies of $\alpha_v\beta_3$ and $\alpha_v\beta_5$ expressing macrophages were significantly decreased compared to untreated cells (Fig. 3C, D, E, F, Supplemental Fig. 2D). However, the *de novo* expression of these integrins at mRNA levels were unchanged following treatment of macrophages with NETs (Supplemental Fig. 3A–C). We further assessed extracellular levels of one of these integrins and found significant increase in the levels of soluble $\alpha_v\beta_3$ integrin in the NET-stimulated macrophages compared to untreated control, indicating that NETs cause cleavage of the integrin to be released to the extracellular space (Supplemental Fig. 3D).

NE present in NETs decreases surface levels of integrins to inhibit efferocytosis

NETs contain extracellular web-like DNA structures. Treatment of macrophages and apoptotic cells with NETs significantly inhibited macrophage efferocytosis compared to un-treated control (Fig. 4A, B, Supplemental Fig. 2E). Surprisingly, when macrophage and apoptotic cell cultures were treated with NETs in presence of DNase I which degrades DNA, NET-dependent inhibition of efferocytosis was not corrected as the efferocytosis was still significantly decreased compared to normal un-treated condition (Fig. 4A, B, Supplemental Fig. 2E). This indicated that NET-dependent inhibition of macrophage efferocytosis did not depend on the extracellular DNA of NETs, but possibly on their DNA coating molecules. We found that treatment of macrophages with NETs cleaved integrins (Supplemental Fig. 3D), indicating the possible role of proteases present in the NETs. NE, which is present in the NETs acts as an enzyme to cleave proteins(25). We therefore treated macrophages with recombinant human (rh) NE and assessed $\alpha_v\beta_3$ and $\alpha_v\beta_5$ integrins on the cell surface of macrophages. We found that treatment of macrophages with rhNE significantly decreased the expression of $\alpha_v\beta_3$ and $\alpha_v\beta_5$ integrins on their cell surface compared to untreated macrophages (Fig. 4C, D, E, F, Supplemental Fig. 2F). The *de novo* expression of these integrins at mRNA levels were unaltered following treatment of the macrophages with rhNE (Supplemental Fig. 3A–C); while we noticed significant increase in the levels of soluble $\alpha_v\beta_3$ integrin in the culture supernatants after treatment of macrophages with rhNE compared to PBS-treated macrophages (Supplemental Fig. 3D). We further correlated the decreased surface $\alpha_v\beta_3$ and $\alpha_v\beta_5$ integrins in macrophages with the decreased frequencies of macrophage efferocytosis following treatment of macrophages with rhNE in a dose-dependent manner (Fig. 4G, I, Supplemental Fig. 2G). By contrast, treatment of macrophages with an NE inhibitor significantly rescued rhNE-dependent inhibition of macrophage efferocytosis (Fig. 4H, J, Supplemental Fig. 2G). These data clearly suggest

that NE present on the NETs reduces macrophage efferocytosis by disrupting and cleaving $\alpha_v\beta_3$ and $\alpha_v\beta_5$ integrins on macrophages.

Blockade of NE reverses eCIRP-induced NET-dependent inhibition of efferocytosis

We next assessed the effects of an NE inhibitor on eCIRP-induced NET-dependent inhibition of macrophage efferocytosis. We found that macrophages cultured with apoptotic cells in the presence of NETs significantly decreased efferocytosis compared to untreated control (Fig. 5A, B). However, treatment with NE inhibitor to this culture increased the efferocytosis in a dose-dependent manner in the presence of NETs quantitatively (Fig. 5A, B) and qualitatively (Fig. 5C). Thus, targeting NE opposes NET-dependent inhibition of macrophage efferocytosis.

eCIRP deficiency increases efferocytosis in sepsis

We previously showed that CIRP deficient mice had decreased levels of NETs in the blood and lungs after sepsis(19). Here, we assessed macrophage efferocytosis in the peritoneal cavity of WT and $CIRP^{-/-}$ mice in sepsis. We found that the frequencies of macrophage efferocytosis in the peritoneal cavity of WT mice was decreased significantly in sepsis compared to sham mice (Fig. 6A, B). However, in $CIRP^{-/-}$ mice the frequencies of peritoneal macrophage efferocytosis in sepsis was significantly increased compared to WT septic mice (Fig. 6A, B). These data indicate that blocking eCIRP protects mice from NET-dependent inhibition of efferocytosis. In the peritoneal cavity there are macrophages, lymphocytes, and neutrophils. The cells which remained at the same FSC, but F4/80 negative could be the lymphocytes or granulocytes.

Discussion

Apoptotic cells are engulfed by the macrophages to maintain cellular homeostasis. Unengulfed apoptotic cells may undergo secondary necrosis, releasing intracellular molecules to cause tissue injury(6–8). eCIRP, a novel DAMP released during inflammatory diseases such as sepsis activates immune cells through TLR4, further fueling inflammation(13, 26). NETs trap and kill bacteria, but uncontrolled NET formation causes severe inflammation and organ injury in sepsis(15, 16). While NETs activate immune cells to release pro-inflammatory cytokines(27, 28), their effect on macrophage efferocytosis has not been studied yet. In this study, we have identified an unique role of eCIRP-induced NETs to inhibit phagocytosis of apoptotic cells by the macrophages through a novel mechanism (Fig. 7). We identified that NE present in the NETs cleaved $\alpha_v\beta_3$ and $\alpha_v\beta_5$ integrins expressed on macrophages which recognize apoptotic cell's opsonin MFG-E8, thereby inhibiting macrophage efferocytosis. This novel relationship between eCIRP-induced NETs and efferocytosis was confirmed in murine sterile inflammation induced by *in vivo* rmCIRP injection, as well as in a pre-clinical murine model of sepsis. We found that targeting CIRP using $CIRP^{-/-}$ mice corrected NET-dependent impairment of efferocytosis in sepsis.

Neutrophils treated with 1 μg/mL of rmCIRP produced 20 μg/mL NETs. Interestingly, only 100 ng/mL of NETs could significantly inhibit efferocytosis. In murine and human sepsis,

eCIRP levels in the serum were 600 ng/mL and 2 ng/mL, respectively(13, 29). This indicates that due to the elevated release of eCIRP in the serum during sepsis, considerable amounts of NETs can be produced(19, 30). Therefore, the concentration of NETs used to determine its effects on efferocytosis is physiologically relevant. A wide range of stimuli, such as bacteria, virus, fungi, PMA, IL-8, and LPS induce NET formation(27). DAMPs such as HMGB1 has been shown to induce NET formation(31). We have recently discovered that eCIRP induces NET formation through PAD4 activation(19). Current study proved that NETs played a pivotal role in inhibiting macrophage efferocytosis following eCIRP treatment, because stimulation of PAD4$^{-/-}$ PMN or injection in PAD4$^{-/-}$ mice with rmCIRP did not attenuate macrophage efferocytosis. NETs contain extracellular chromatin decorated with citrulinated H3, MPO, NE(14). We found that the inhibition of efferocytosis by PMA-induced NETs was not as profound as the effects of eCIRP-induced NETs. The differential outcomes of eCIRP- vs PMA-induced NETs on efferocytosis could be due to the presence of different components at varied quantities in the NETs isolated from eCIRP and PMA treated neutrophils. Since eCIRP induces the generation of a distinct type of neutrophils, ICAM-1^{+} neutrophils(20), it is likely that the NETs released by rmCIRP treatment may have unique composition, exhibiting distinct impacts on efferocytosis. In support of our current finding, a recent study revealed that NETs components vary among various stimulants of NET induction(32). Since several stimuli have been shown to induce NET formation, further studies to define whether or not NETs induced by various stimuli other than eCIRP can exhibit inhibitory effects on efferocytosis.

PAD4$^{-/-}$ mice had decreased levels of NETs(22, 33). The types of molecules present in the NETs in WT vs PAD4$^{-/-}$ mice neutrophils are unknown. We co-cultured WT or PAD4$^{-/-}$ PMN with macrophages and treated with rmCIRP. As a result of the decreased production of NETs by the PAD4$^{-/-}$ neutrophils the efferocytosis was significantly higher compared to WT neutrophils co-cultured with macrophages and apoptotic cells and treatment with rmCIRP. Akin to our current approach, if we had isolated the NETs from rmCIRP-treated PAD4$^{-/-}$ neutrophils and added to the culture, we would have seen the similar results of higher efferocytosis than the NETs from WT neutrophils. The higher the NETs added to the culture, the lower the efferocytosis would be. Thus, to exclude bias, we used the strategy to add neutrophils from WT and PAD4$^{-/-}$ mice and co-cultured them with macrophages and apoptotic cells and assessed phagocytosis. Nonetheless, the presence of neutrophils in the co-culture would add several and uncontrolled factors released by these cells. Since rmCIRP treatment of WT and PAD4$^{-/-}$ mice showed similar numbers of macrophages and neutrophils in the peritoneal cavity, the presence of unknown factors in the PMN of both strains of mice could be the same.

It has been shown that DAMPs such as H3 and HMGB1 inhibit efferocytosis(34–37). These molecules are also present in NETs. H3 is present in NETs as citrulinated form (citH3) because PAD4 activation during NETosis alters H3's arginine to citruline, thus pointing to a concern whether or not the citH3 affects efferocytosis to the same extent of naïve H3. HMGB1 may undergo extensive post-translational modifications, including reversible and terminal cysteine oxidation, acetylation, methylation, ADP ribosylation, glycation, and phosphorylation(38). Some of these modifications have been demonstrated to influence on their biological functions. Although it has been shown that HMGB1 inhibits efferocytosis,

which form of HMGB1 is present in the NETs and whether or not various post-translationally modified forms of HMGB1 have diverse effects on efferocytosis are not known. Similarly, it is still unknown whether or not NETs contain eCIRP which may inhibit efferocytosis. To address this we performed an experiment by treating macrophages with rmCIRP and then assessed macrophage efferocytosis. We found that treatment of macrophages with eCIRP alone did not affect efferocytosis, suggesting that even if NETs contain eCIRP, it may not affect effeocytosis. We further revealed that the DNA contained in the NETs did not alter normal efferocytosis, as DNAse treatment could not restore the inhibition of efferocytosis caused by NETs, indicating that it is not DNA but other molecules contained in the DNA inhibit efferocytosis.

Several molecules acting as opsonins of apoptotic cells promote efferocytosis(4, 7). MFG-E8 is an opsonin which promotes engulfment of apoptotic cells by the macrophages and protects host from inflammatory and autoimmune diseases(10, 11). Surprisingly, we found that eCIRP-induced NET-dependent inhibition of efferocytosis was not corrected even in the presence of MFG-E8, indicating the possible disruption of MFG-E8 and its receptor(s)-mediated pathway for efferocytosis. This unexpected finding led us to focus on its receptors $\alpha_v\beta_3$ and $\alpha_v\beta_5$ integrins. We found decreased levels of these integrins in the surface of macrophages after treatment with NETs. In addition to H3, MPO, and HMGB1, the proteinase NE is present in NETs. NE cleaves a wide range of proteins. We previously showed that NE cleaves junctional adhesion molecule-C (JAM-C) of endothelial cells to promote neutrophil's reverse migration(25). Here we showed that macrophages treated with rhNE significantly decreased the surface levels of $\alpha_v\beta_3$ and $\alpha_v\beta_5$ integrins, while treatment with the inhibitor of NE protected cells from rmNE-dependent surface integrin cleavage. To get deeper insights into the involvement of NE of NETs to cause inhibition of efferocytosis, we treated cells with NETs and NE inhibitor and found that NE inhibitor significantly corrected the inhibition of efferocytosis by the NETs. This novel role of NE to disrupt integrins for inhibiting efferocytosis rewrites the pathophysiology of inflammatory diseases and directs new therapeutic avenues. Since a number of scavenger receptors and their ligands are involved in efferocytosis, future studies on the effects of NE on other receptors would be of great interest.

We transformed these *in vitro* findings in murine sepsis, which is characterized by increased rate of cellular apoptosis(3). We found that $CIRP^{-/-}$ mice had increased rate of efferocytosis in the peritoneal cavity than WT mice in sepsis. Besides efferocytosis, clearance of bacteria by the phagocytes is also important in resolving infection. This novel discovery of the inhibitory role of eCIRP-induced NETs to impair phagocytic clearance of apoptotic cells can be implemented in elucidating the role of NETs on phagocytic clearance of bacteria by professional phagocytes. This important physiological function can further be linked with the immunoregulatory phenomenon as determined by the release of anti-inflammatory cytokines and the ability of antigen presenting cells to engulf pathogen, digest them, and present to T cells for enabling adaptive functions.

Our previous study showed increased levels of NETs in the lungs in rmCIRP-treated animals(19). During sepsis, endothelial cell damage and epithelial cell apoptosis occur in the lungs, attributing their immediate clearance to resolve inflammation and tissue injury, which

eventually be hampered by the presence of eCIRP-induced NETs in the tissues. In addition to the lungs, focusing on other organs in which neutrophil infiltration, NET formation, and cellular apoptosis simultaneously take place will be the possible candidates to study the role of eCIRP-induced NETs on efferocytosis in various disease models. Our current discovery elucidating a novel role of eCIRP-induced NETs in murine cells and disease models may shed lights on the mechanisms of pathogenesis of inflammatory diseases.

Supplementary Material

Refer to Web version on PubMed Central for supplementary material.

Acknowledgements

We thank Mahendar Ochani of the center for immunology and inflammation, Feinstein Institutes for Medical Research for providing technical support in animal experiments.

Grants support

This study was supported by the National Institutes of Health (NIH) grants R35GM118337 (P.W.), R01HL076179 (P.W.), and R01GM129633 (M.A.) and Shock Society faculty award grant (M.A.).

Abbreviations

eCIRP	extracellular cold-inducible RNA-binding protein
DAMP	damage-associated molecular pattern
NETs	neutrophil extracellular traps
PAD4	peptidyl arginine deaminase 4
MFG-E8	milk fat globule-EGF-factor VIII
NE	neutrophil elastase
PAMPs	pathogen-associated molecular patterns
PS	phosphatidylserine
TLR4	Toll-like receptor 4
MPO	myeloperoxidase
GSDMD	gasdermin D
PMA	phorbol myristate acetate
CLP	cecal ligation and puncture
BMDN	bone marrow-derived neutrophils
JAM-C	junctional adhesion molecule-C
CFSE	carboxyfluorescein succinimidyl ester

References

1. Singer M, Deutschman CS, Seymour CW, Shankar-Hari M, Annane D, Bauer M, Bellomo R, Bernard GR, Chiche JD, Coopersmith CM, Hotchkiss RS, Levy MM, Marshall JC, Martin GS, Opal SM, Rubenfeld GD, van der Poll T, Vincent JL, and Angus DC. 2016 The Third International Consensus Definitions for Sepsis and Septic Shock (Sepsis-3). JAMA 315: 801–810. [PubMed: 26903338]
2. Aziz M, Jacob A, Yang WL, Matsuda A, and Wang P. 2013 Current trends in inflammatory and immunomodulatory mediators in sepsis. J Leukoc Biol 93: 329–342. [PubMed: 23136259]
3. Wesche DE, Lomas-Neira JL, Perl M, Chung CS, and Ayala A. 2005 Leukocyte apoptosis and its significance in sepsis and shock. J Leukoc Biol 78: 325–337. [PubMed: 15817707]
4. Elliott MR, Koster KM, and Murphy PS. 2017 Efferocytosis Signaling in the Regulation of Macrophage Inflammatory Responses. J Immunol 198: 1387–1394. [PubMed: 28167649]
5. Proto JD, Doran AC, Gusarova G, Yurdagul A, Sozen E, Subramanian M, Islam MN, Rymond CC, Du J, Hook J, Kuriakose G, Bhattacharya J, and Tabas I. 2018 Regulatory T Cells Promote Macrophage Efferocytosis during Inflammation Resolution. Immunity 49: 666–677.e666. [PubMed: 30291029]
6. Sachet M, Liang YY, and Oehler R. 2017 The immune response to secondary necrotic cells. Apoptosis 22: 1189–1204. [PubMed: 28861714]
7. Elliott MR, and Ravichandran KS. 2016 The Dynamics of Apoptotic Cell Clearance. Dev Cell 38: 147–160. [PubMed: 27459067]
8. Arandjelovic S, and Ravichandran KS. 2015 Phagocytosis of apoptotic cells in homeostasis. Nat Immunol 16: 907–917. [PubMed: 26287597]
9. Segawa K, and Nagata S. 2015 An Apoptotic 'Eat Me' Signal: Phosphatidylserine Exposure. Trends Cell Biol 25: 639–650. [PubMed: 26437594]
10. Hanayama R, Tanaka M, Miwa K, Shinohara A, Iwamatsu A, and Nagata S. 2002 Identification of a factor that links apoptotic cells to phagocytes. Nature 417: 182–187. [PubMed: 12000961]
11. Aziz M, Jacob A, Matsuda A, and Wang P. 2011 Review: milk fat globule-EGF factor 8 expression, function and plausible signal transduction in resolving inflammation. Apoptosis 16: 1077–1086. [PubMed: 21901532]
12. Nishiyama H, Itoh K, Kaneko Y, Kishishita M, Yoshida O, and Fujita J. 1997 A glycine-rich RNA-binding protein mediating cold-inducible suppression of mammalian cell growth. J Cell Biol 137: 899–908. [PubMed: 9151692]
13. Qiang X, Yang WL, Wu R, Zhou M, Jacob A, Dong W, Kuncewitch M, Ji Y, Yang H, Wang H, Fujita J, Nicastro J, Coppa GF, Tracey KJ, and Wang P. 2013 Cold-inducible RNA-binding protein (CIRP) triggers inflammatory responses in hemorrhagic shock and sepsis. Nat Med 19: 1489–1495. [PubMed: 24097189]
14. Brinkmann V, Reichard U, Goosmann C, Fauler B, Uhlemann Y, Weiss DS, Weinrauch Y, and Zychlinsky A. 2004 Neutrophil extracellular traps kill bacteria. Science 303: 1532–1535. [PubMed: 15001782]
15. Kaplan MJ, and Radic M. 2012 Neutrophil extracellular traps: double-edged swords of innate immunity. J Immunol 189: 2689–2695. [PubMed: 22956760]
16. Yang H, Biermann MH, Brauner JM, Liu Y, Zhao Y, and Herrmann M. 2016 New Insights into Neutrophil Extracellular Traps: Mechanisms of Formation and Role in Inflammation. Front Immunol 7: 302. [PubMed: 27570525]
17. Sollberger G, Choidas A, Burn GL, Habenberger P, Di Lucrezia R, Kordes S, Menninger S, Eickhoff J, Nussbaumer P, Klebl B, Krüger R, Herzig A, and Zychlinsky A. 2018 Gasdermin D plays a vital role in the generation of neutrophil extracellular traps. Sci Immunol 3.
18. Brinkmann V 2018 Neutrophil Extracellular Traps in the Second Decade. J Innate Immun 10: 414–421. [PubMed: 29909412]
19. Ode Y, Aziz M, Jin H, Arif A, Nicastro JG, and Wang P. 2019 Cold-inducible RNA-binding Protein Induces Neutrophil Extracellular Traps in the Lungs during Sepsis. Sci Rep 9: 6252. [PubMed: 31000768]

20. Ode Y, Aziz M, and Wang P. 2018 CIRP increases ICAM-1^{+} phenotype of neutrophils exhibiting elevated iNOS and NETs in sepsis. J Leukoc Biol 103: 693–707. [PubMed: 29345380]
21. Aziz M, Yang WL, and Wang P. 2013 Measurement of phagocytic engulfment of apoptotic cells by macrophages using pHrodo succinimidyl ester. Curr Protoc Immunol Chapter 14: Unit 14 31.
22. Rohrbach AS, Slade DJ, Thompson PR, and Mowen KA. 2012 Activation of PAD4 in NET formation. Front Immunol 3: 360. [PubMed: 23264775]
23. Mestas J, and Hughes CC. 2004 Of mice and not men: differences between mouse and human immunology. J Immunol 172: 2731–2738. [PubMed: 14978070]
24. Eruslanov EB, Singhal S, and Albelda SM. 2017 Mouse versus Human Neutrophils in Cancer: A Major Knowledge Gap. Trends Cancer 3: 149–160. [PubMed: 28718445]
25. Jin H, Aziz M, Ode Y, and Wang P. 2018 Cirp Induces Neutrophil Reverse Transendothelial Migration in Sepsis. Shock.
26. Aziz M, Brenner M, and Wang P. 2019 Extracellular CIRP (eCIRP) and inflammation. J Leukoc Biol 106: 133–146. [PubMed: 30645013]
27. Delgado-Rizo V, Martínez-Guzmán MA, Iñiguez-Gutierrez L, García-Orozco A, Alvarado-Navarro A, and Fafutis-Morris M. 2017 Neutrophil Extracellular Traps and Its Implications in Inflammation: An Overview. Front Immunol 8: 81. [PubMed: 28220120]
28. Papayannopoulos V 2018 Neutrophil extracellular traps in immunity and disease. Nat Rev Immunol 18: 134–147. [PubMed: 28990587]
29. Gurien SD, Aziz M, Jin H, Wang H, He M, Al-Abed Y, Nicastro JM, Coppa GF, and Wang P. 2019 Extracellular microRNA 130b-3p inhibits eCIRP-induced inflammation. EMBO Rep: e48075. [PubMed: 31724825]
30. Murao A, Arif A, Brenner M, Denning NL, Jin H, Takizawa S, Nicastro B, Wang P, and Aziz M. 2020 Extracellular CIRP and TREM-1 axis promotes ICAM-1-Rho-mediated NETosis in sepsis. FASEB J 34: 9771–9786. [PubMed: 32506691]
31. Tadie JM, Bae HB, Jiang S, Park DW, Bell CP, Yang H, Pittet JF, Tracey K, Thannickal VJ, Abraham E, and Zmijewski JW. 2013 HMGB1 promotes neutrophil extracellular trap formation through interactions with Toll-like receptor 4. Am J Physiol Lung Cell Mol Physiol 304: L342–349. [PubMed: 23316068]
32. Petretto A, Bruschi M, Pratesi F, Croia C, Candiano G, Ghiggeri G, and Migliorini P. 2019 Neutrophil extracellular traps (NET) induced by different stimuli: A comparative proteomic analysis. PLoS One 14: e0218946. [PubMed: 31283757]
33. Biron BM, Chung CS, Chen Y, Wilson Z, Fallon EA, Reichner JS, and Ayala A. 2018 PAD4 Deficiency Leads to Decreased Organ Dysfunction and Improved Survival in a Dual Insult Model of Hemorrhagic Shock and Sepsis. J Immunol 200: 1817–1828. [PubMed: 29374076]
34. Grégoire M, Uhel F, Lesouhaitier M, Gacouin A, Guirriec M, Mourcin F, Dumontet E, Chalin A, Samson M, Berthelot LL, Tissot A, Kerjouan M, Jouneau S, Le Tulzo Y, Tarte K, Zmijewski JW, and Tadié JM. 2018 Impaired efferocytosis and neutrophil extracellular trap clearance by macrophages in ARDS. Eur Respir J 52.
35. Liu G, Wang J, Park YJ, Tsuruta Y, Lorne EF, Zhao X, and Abraham E. 2008 High mobility group protein-1 inhibits phagocytosis of apoptotic neutrophils through binding to phosphatidylserine. J Immunol 181: 4240–4246. [PubMed: 18768881]
36. Friggeri A, Yang Y, Banerjee S, Park YJ, Liu G, and Abraham E. 2010 HMGB1 inhibits macrophage activity in efferocytosis through binding to the alphavbeta3-integrin. Am J Physiol Cell Physiol 299: C1267–1276. [PubMed: 20826760]
37. Friggeri A, Banerjee S, Xie N, Cui H, De Freitas A, Zerfaoui M, Dupont H, Abraham E, and Liu G. 2012 Extracellular histones inhibit efferocytosis. Mol Med 18: 825–833. [PubMed: 22495510]
38. Yang H, Antoine DJ, Andersson U, and Tracey KJ. 2013 The many faces of HMGB1: molecular structure-functional activity in inflammation, apoptosis, and chemotaxis. J Leukoc Biol 93: 865–873. [PubMed: 23446148]

Key points

1. eCIRP induces NET formation, causing inhibition of efferocytosis during sepsis.
2. NE of NETs disrupts $\alpha_v\beta_{3/5}$ integrin in macrophages to inhibit efferocytosis.

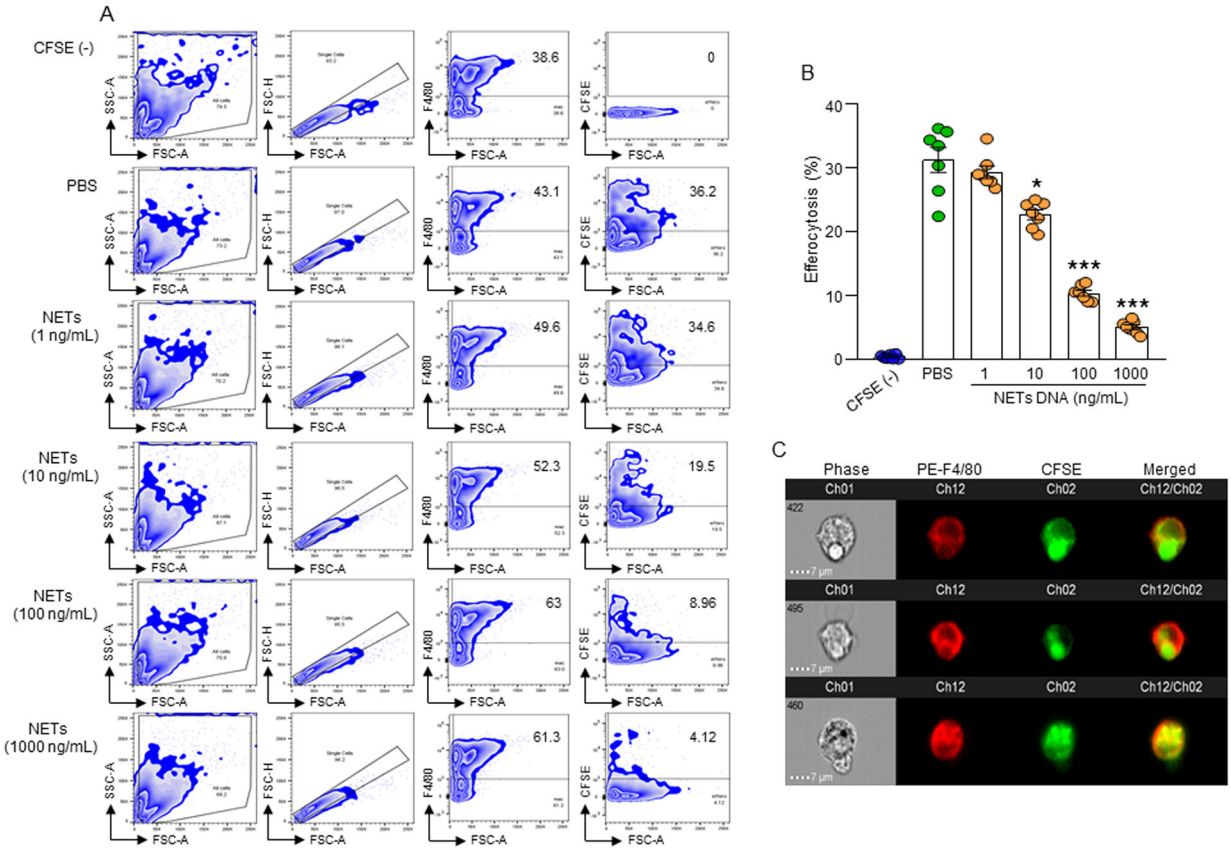

Figure 1: eCIRP-induced NETs inhibit efferocytosis.

(A, B) A total of 5×10^5 peritoneal macrophages were cultured with 1.5×10^6 CFSE-labeled apoptotic cells in presence with PBS or various concentrations of NETs. After 1 h of incubation, cells were washed, fixed with 2% PFA, and efferocytosis was assessed by flow cytometry. Efferocytosis was determined as the percentage of CFSE-positive cells present in $F4/80^+$ macrophages. Data were obtained from 3 independent experiments and expressed as means ± SE (n=7 samples/group). The groups were compared by one-way ANOVA and SNK method (*p<0.05; ***p<0.001 vs. PBS-treated group). **(C)** Confirmation of phagocytosis of apoptotic cells in F4/80 and CFSE double-positive population by image stream analysis. Representative images showing co-localization of F4/80 and CFSE double positive cells indicate efferocytosis. Scale bar: 7 μm. BMDN, bone marrow-derived neutrophil(s); MPO, myeloperoxidase; CFSE, carboxyfluorescein succinimidyl ester; PFA, paraformaldehyde; NETs, neutrophil extracellular traps; rmCIRP, recombinant mouse cold-inducible RNA-binding protein.

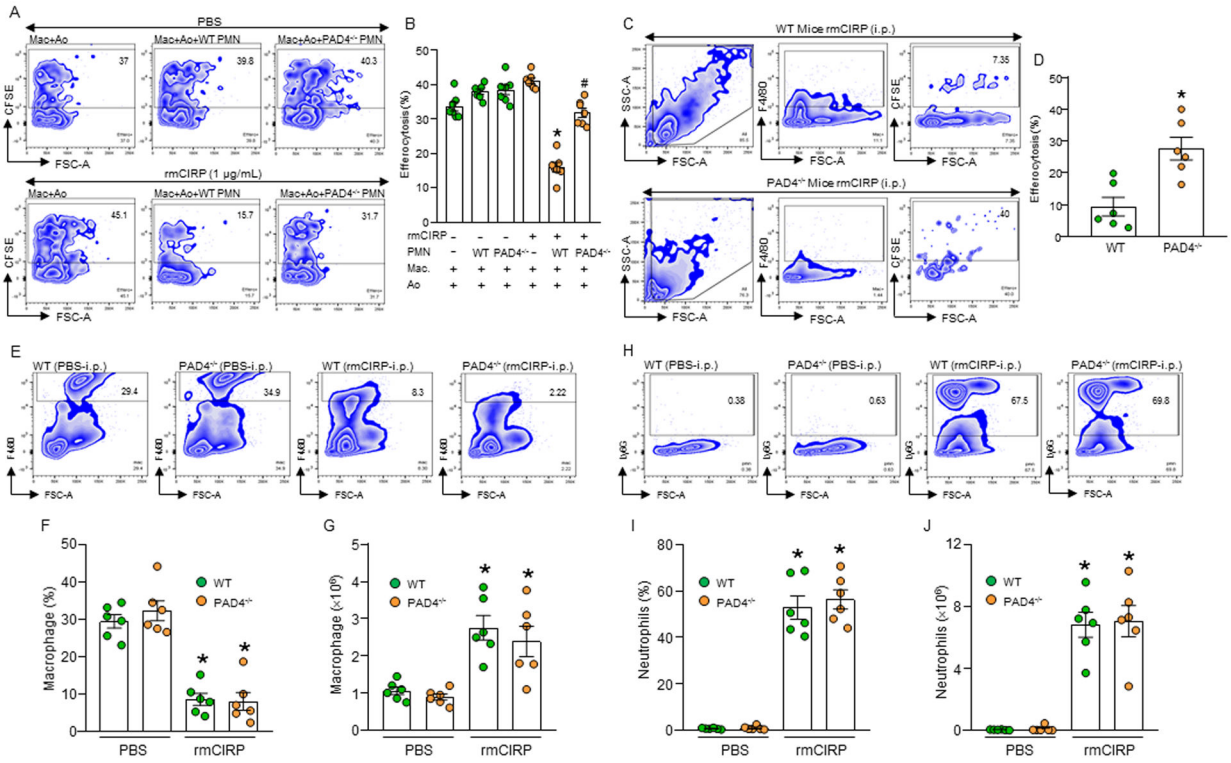

Figure 2: eCIRP-induced wild-type, but not PAD4$^{-/-}$ neutrophils inhibit efferocytosis.

(A, B) BMDN (1× 10^6) isolated from WT or PAD4$^{-/-}$ mice were stimulated with PBS or rmCIRP (1 μg/mL) for 4 h to allow them to form NETs. Peritoneal macrophages (5 × 10^5) and CFSE-labeled apoptotic cells (Ao) (1.5 × 10^6) were separately added to PBS- or rmCIRP-treated WT or PAD4$^{-/-}$ PMN. Cells were continued to culture for 1 h. Cells were then stained with PE-F4/80 Abs and assessed efferocytosis by flow cytometry. Data were obtained from 3 independent experiments and expressed as means ± SE (n=7 samples/group). The groups were compared by one-way ANOVA and SNK method. *p<0.05 vs. rmCIRP(−) PMN(−); #p<0.05 vs. rmCIRP(+) WT PMN(+). **(C, D)** WT and PAD4$^{-/-}$ mice were injected with rmCIRP (5 mg/kg; *i.p.*). After 4 h of injection with rmCIRP, a total of 1 × 10^7 CFSE-labeled apoptotic cells were injected *i.p.* into the mice. After 1 h, peritoneal washout cells were collected, stained with PE-F4/80 Ab, and assessed efferocytosis by flow cytometry. Data were obtained from 3 independent experiments and expressed as means ± SE (n=6 mice/group). The groups were compared by one-way ANOVA and SNK method. *p<0.05 vs. WT mice. **(E-J)** WT and PAD4$^{-/-}$ mice were injected with rmCIRP (5 mg/kg; *i.p.*). After 20 h of injecting the mice with rmCIRP, peritoneal washout cells were harvested and stained with macrophage marker PE-F4/80 and neutrophil marker APC-Ly6G Abs. The contents of **(E-G)** macrophages and **(H-J)** neutrophils in the peritoneal cavity were assessed my flow cytometry. Data were obtained from 3 independent experiments and expressed as means ± SE (n=6 mice/group). The groups were compared by one-way ANOVA and SNK method. *p<0.05 vs. PBS-treated WT/PAD4$^{-/-}$ mice. PAD4, peptidylarginine deiminase 4; PMN, polymorphonuclear leukocytes; Ao, apoptotic cells.

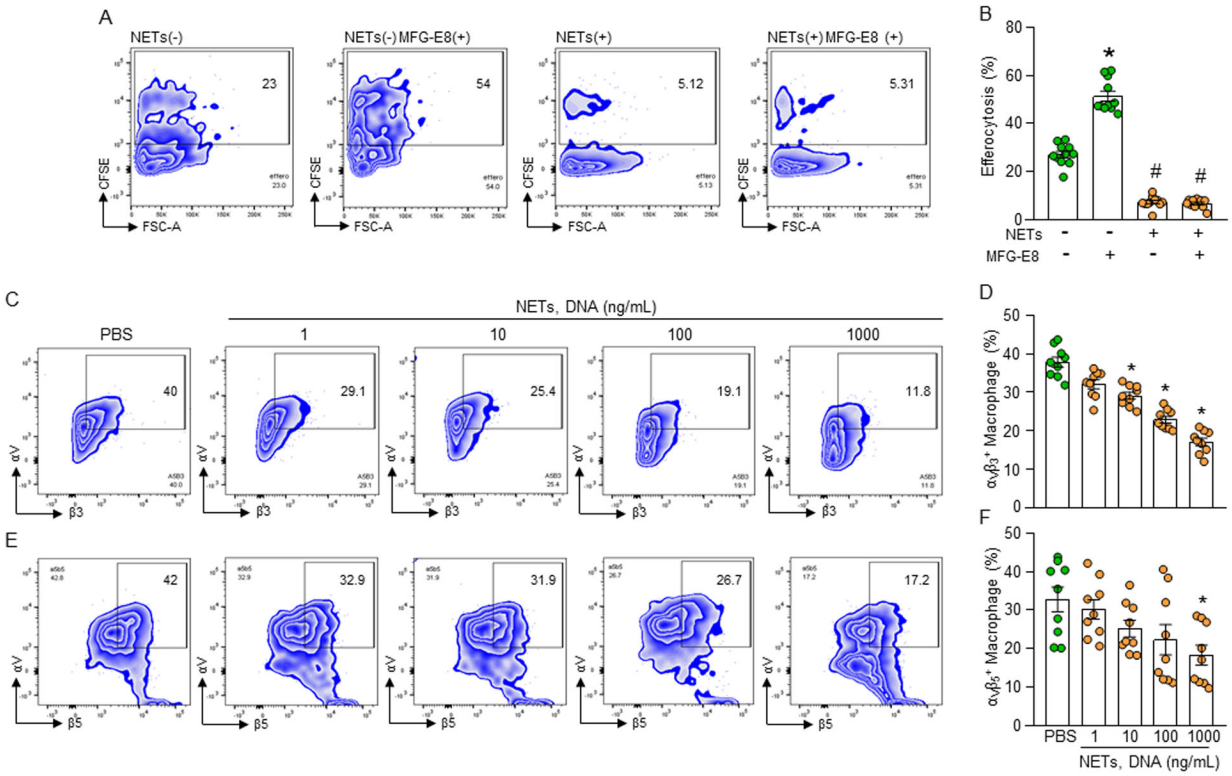

Figure 3: NETs decrease integrin-mediated efferocytosis.

(A, B) Peritoneal macrophages (5×10^5) and CFSE-labeled apoptotic cells (1.5×10^6) in the presence of NETs (1000 ng/mL) with or without rmMFG-E8 (2 μg/mL). After 1 h of incubation, the cells were collected, washed, and stained with PE-F4/80 Ab and assessed efferocytosis in macrophages by flow cytometry. Data were obtained from 3 independent experiments and expressed as means ± SE (n=6 mice/group). The groups were compared by one-way ANOVA and SNK method. *$p<0.05$ vs. NETs(−) rmMFG-E8(−); #$p<0.05$ vs. NETs(−) rmMFG-E8(+). **(C-F)** Impaired surface expression of integrins in NETs-treated macrophages. Peritoneal macrophages (5×10^5) were treated with NETs at various doses. After 1 h of stimulation, the macrophages were washed, stained with **(C, D)** anti- $\alpha_v\beta_3$ and **(E, F)** $\alpha_v\beta_5$ integrin Abs and detected integrins' expression by flow cytometry. Data were obtained from 3 independent experiments and expressed as means ± SE (n=9 samples/group). The groups were compared by one-way ANOVA and SNK method. *$p<0.05$ vs. PBS-treated macrophages. rmMFG-E8, recombinant mouse milk fat globule-EGF-factor VIII.

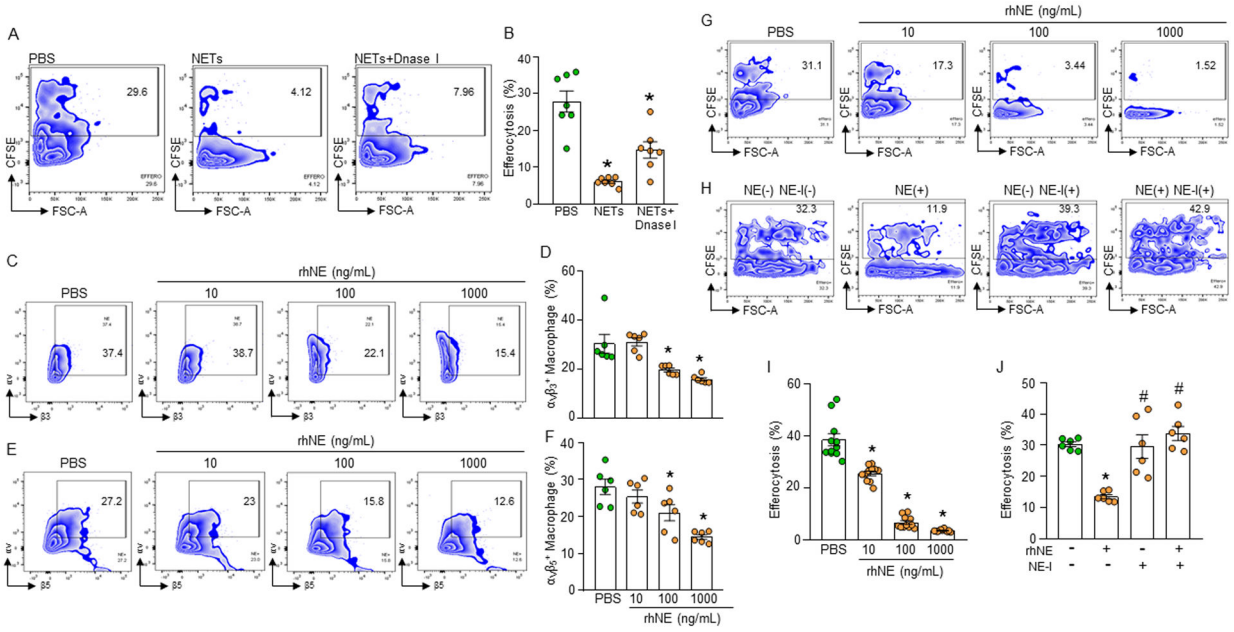

Figure 4: NE cleaves integrins causing impaired efferocytosis.

(A, B) Murine peritoneal macrophages (5×10^5) were cultured with CFSE-stained apoptotic cells (1.5×10^6) in presence of NETs (1000 ng/mL) and DNase I (500U/mL). After 1 h of cell culture, the cells were washed and stained with PE-F4/80 Ab and assessed efferocytosis using flow cytometry. **(C-F)** Assessment of surface expression of integrins following treatment of the macrophages with various doses of rmNE. After treatment of the peritoneal macrophages (5×10^5) with rmNE for 4 h the cells were washed and stained with **(C, D)** anti-$\alpha_v\beta_3$ and **(E, F)** $\alpha_v\beta_5$ integrin Abs and assessed their expression by flow cytometry. **(G, I)** Peritoneal macrophages (5×10^5) and CFSE-labeled apoptotic cells (1.5×10^6) were co-cultured in the presence of various doses of rmNE. After 1 h, the cells were washed and stained with PE-F4/80 Ab and the efferocytosis was assessed by flow cytometry. Data were obtained from 3 independent experiments and expressed as means ± SE (n=7–9 samples/group). The groups were compared by one-way ANOVA and SNK method. *$p<0.05$ vs. PBS-treated macrophages. **(H, J)** Peritoneal macrophages (5×10^5) and CFSE-labeled apoptotic cells (1.5×10^6) were co-cultured in the presence of rmNE (1000 ng/mL) with or without NE-I (100 μM). After 1 h, the cells were washed and stained with PE-F4/80 Ab and assessed efferocytosis by flow cytometry. Data were obtained from 3 independent experiments and expressed as means ± SE (n=6 samples/group). The groups were compared by one-way ANOVA and SNK method. *$p<0.05$ vs. NE(−) NE-I(−); #$p<0.05$ vs. NE(+) NE-I(−). NE, neutrophil elastase; NE-I, NE-inhibitor.

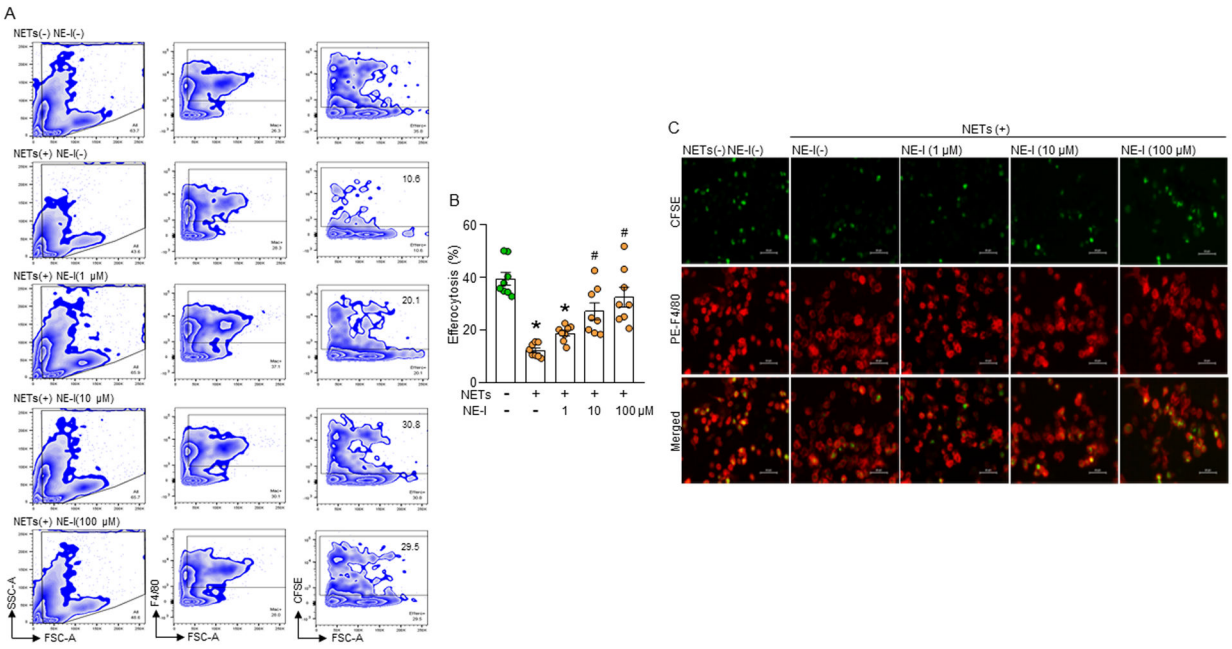

Figure 5: NE inhibitor reverses NET-dependent impairment of efferocytosis.

(A, B) Murine peritoneal macrophages (5×10^5) and CFSE-labeled apoptotic cells (1.5×10^6) in presence of NETs (1000 ng/mL) and various doses of NE-I. After 1 h of cell culture, the cells were washed and stained with PE-F4/80 Ab and assessed efferocytosis using flow cytometry. Data were obtained from 3 independent experiments and expressed as means ± SE (n=8 samples/group). The groups were compared by one-way ANOVA and SNK method. *p<0.05 vs. NETs(−) NE-I(−); #p<0.05 vs. NETs(+) NE-I(–). **(C)** Murine peritoneal macrophages (5×10^5) were plated in 24-well plate. CFSE-stained apoptotic cells (1.5×10^6) were added to the macrophages. The cells were treated with NETs (1000 ng/mL) and various doses of NE-I. After 1 h of incubation, media was carefully removed, washed the cells with PBS, followed by fixing and stained the cells with PE-F4/80 Ab. Efferocytosis was detected by using fluorescent microscope at ×400 original magnification. Representative images in each group were chosen from 10 randomly captured images. Scale bar: 40 μm.

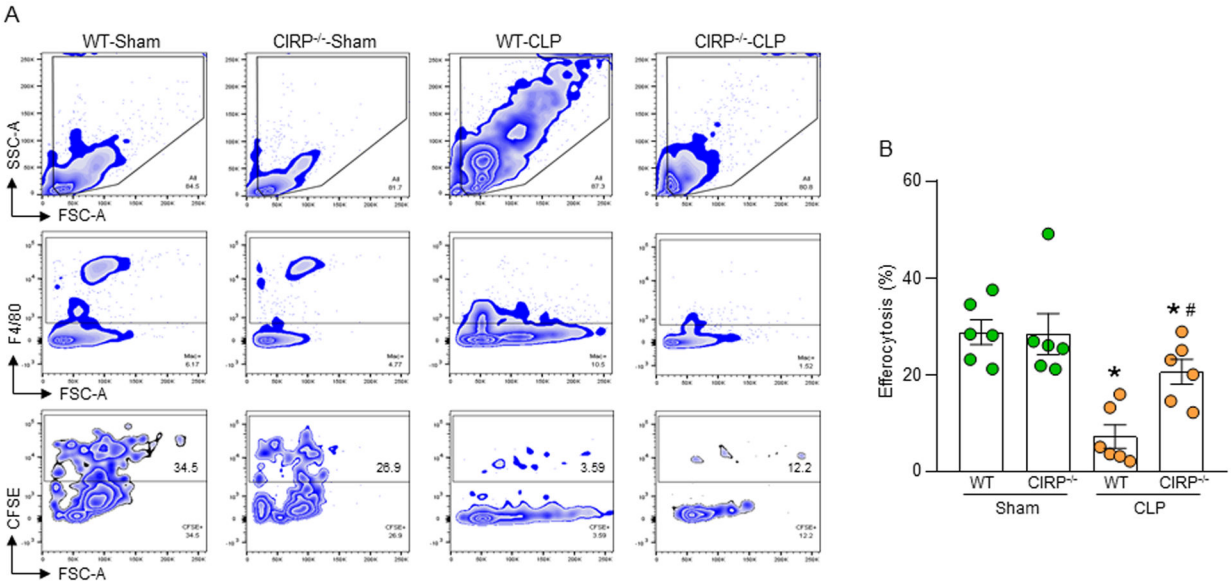

Figure 6: CIRP$^{-/-}$ mice have increased efferocytosis in sepsis.

(A, B) WT and CIRP$^{-/-}$ mice were underwent sham and CLP operation. After 5 h of surgery all mice were injected with CFSE-labeled apoptotic cells (1×10^7) via *i.p.* injection. After 1 h of injection of apoptotic cells, peritoneal washout cells were collected and stained with PE-F4/80 Ab and assessed efferocytosis by flow cytometry. Data were obtained from 3 independent experiments are expressed as means ± SE (n=6 mice/group). The groups were compared by one-way ANOVA and SNK method. *p<0.05 vs. relevant (WT or CIRP$^{-/-}$) sham mice; #p<0.05 vs. WT CLP mice.

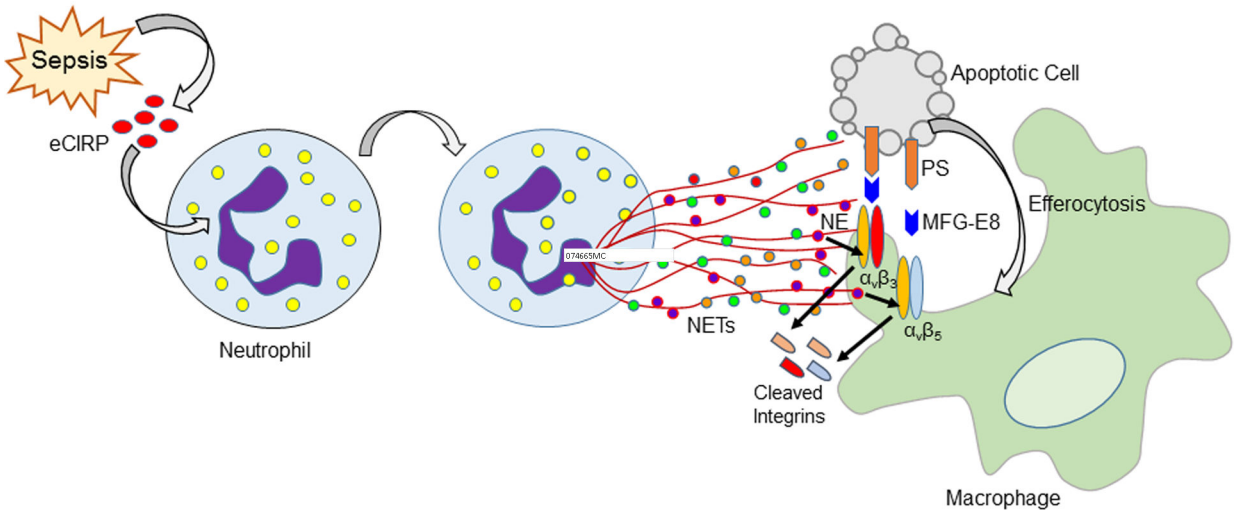

Figure 7: Schematic Summary.

eCIRP is released during sepsis, which induces neutrophils to produce NETs. NE contained in the NETs cleaves $\alpha_v\beta_3$ and $\alpha_v\beta_5$ integrins expressed on the surface of macrophages. This leads to decreased binding of apoptotic cell's opsonin MFG-E8 to the macrophage, thereby impairing the bridge formation between apoptotic cell and macrophage and inhibiting efferocytosis.